Real time Implementation of Sliding mode Based Direct and Indirect Current Control Techniques for Shunt Active Power Filter

Rajesh K Patjoshi, Kamalakanta Mahapatra, Venkata Ratnam Kolluru
Electronics and Communication Engg.Dept.
National Institute of Technology Rourkela, India
rajeshpatjoshi1@gmail.com

Abstract— This paper presents a new and efficient control algorithm which adopted the voltage source inverter to decrease current harmonics generated by the nonlinear load. The sliding mode control (SMC) is employed with the current control loop to achieve fast dynamics control and a simple proportional-integral (PI) controller is adopted in the outer voltage control loop to achieve slow dynamics control. The proposed scheme implements simplified control algorithms depending on the direct current control (DCC) and indirect current control (ICC) techniques for designing trajectories in sliding mode control based shunt active power filter (SAPF). The performances of the DCC and ICC techniques were verified through a simulation with MATLAB-SIMULINK and real-time implementation in Opal RT-Lab. A comparison has been made between the two configurations showing their topological contrasts and load compensation capabilities under ideal, unbalanced and distorted source voltage conditions.

Keywords- current harmonics, fast dynamics, SMC, DCC, ICC, SAP, Real-time.

1 Introduction

With the growing and development of modern industry, a various nonlinear and time-varying electronic devices such as inverters, rectifiers, and switching power supplies are widely utilized. These solid-state converters inject harmonics into the power lines and result in serious distortion in the supply current and voltage and decrease the power quality (PQ) [1,2]. This PQ problem provides low efficiency to the distribution line by increasing current and voltage distortions, excessive neutral current and poor power factor.

The shunt active power filter (SAPF) has become established with assorted structures and topologies main aim to reduce the current harmonics and reactive power in the power system and enhance the PQ. The continuous development of SAPF can provide different current control techniques and grid synchronization techniques [3,4]. Focusing on the current reference tracking of SAPF, many control methods [5,6,7,8,9]-[10] have been proposed in the literature. The current tracking control can be decided by the dynamic behaviour of SAPF, under various operating conditions. As per [11], two types of current control techniques using sliding mode techniques are compared, and find that active power filter with indirect current control (ICC) technique has a simpler structure and better harmonic treating effect than direct current control (DCC). But this method does not provide any dynamic behaviour of SAPF. Active power filter using the indirect current control method is designed in [12,13]. It does not need compensation current and only considers the supply voltage, source current i_{sa} and DC-link voltage v_{dc}. Therefore, such technique can effectively reduce the current harmonics in balanced supply condition. The reference currents tracking behaviour are enhanced by novel sliding mode control, which can reduce the supply current harmonic content in [14]. Here an integer part of the traditional hysteresis control method is added and reduces the steady tracking error by the designed sliding mode controller. Adaptive sliding mode control method [15] is based on tracking error of harmonics and APF [16] current function in the controller and analysed the robustness and stability of the system is analysed by the simulation analysis.

Fuzzy logic-based robust active [17,18]power filter to minimize the harmonics for a wide range of variation of load current under stochastic conditions is considered in-.Sliding mode control can be a high-speed switching feedback control which chooses the suitable switching configuration of the converter like a function of the instantaneous state variables in order to drive the state trajectory onto a switching surface [19,20]. Thus, this control exhibits excellent performance and provides superior tracking performance in all operating conditions.

In this paper, a novel sliding mode controller is implemented in SAPF for tracking reference currents using ICC and DCC methods, in balanced, unbalanced as well as distorted voltage condition, and the performance of SAPF is analysed with total harmonic

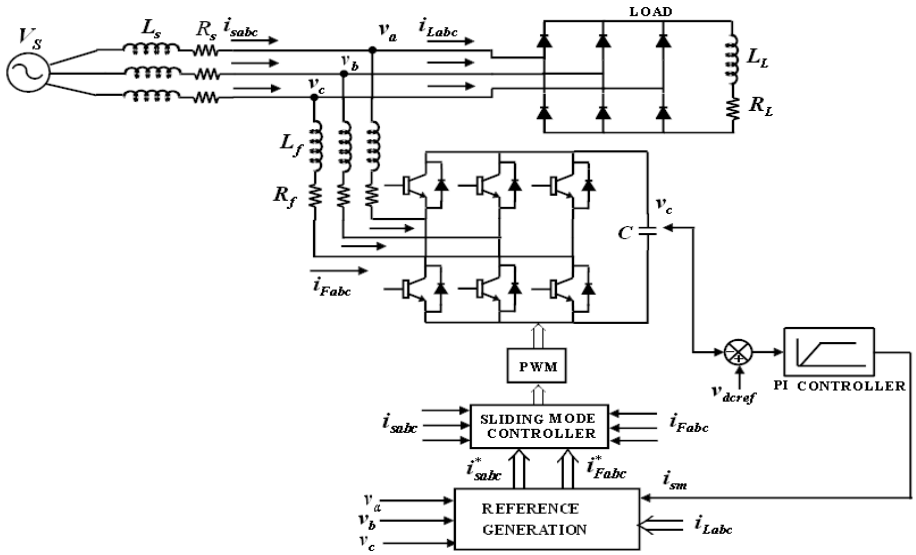

Fig.1 Functional block diagram of SAPF

distortion (THD) of source current in the above three operating conditions of supply voltage. Here MATLAB-SIMULINK results are validated with real-time performance analysis in the RT-LAB simulator. It is one of the most promising real-time simulation tools for all practical applications.

Organization of the paper is as follows: Section II focuses on the development of shunt active power filter with the control strategy of active power filter. In Section III the performances of DCC and ICC are analyzed by means of a simulation platform with MATLAB-SIMULINK. In Section IV real time Opal-RT results are presented. Finally, the most relevant conclusions of this paper are summarized in Section V.

2 Development of Shunt Active Power Filter

The functional diagram of a shunt active power filter, based on a voltage source converter, for the compensation of current harmonics generated by the nonlinear load is shown in Fig.1. A three phase voltage source inverter is employed as a shunt active power filter. The inverter is controlled through two controllers. A fast inner loop is used to control the shape of the line currents, forcing them to be of the same shape, and in phase with, the phase voltages. The inner current loop is based on a sliding-mode controller, which is conceptually

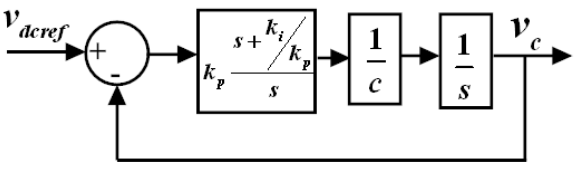

Fig.2 Outer control loop for dc-link voltage control

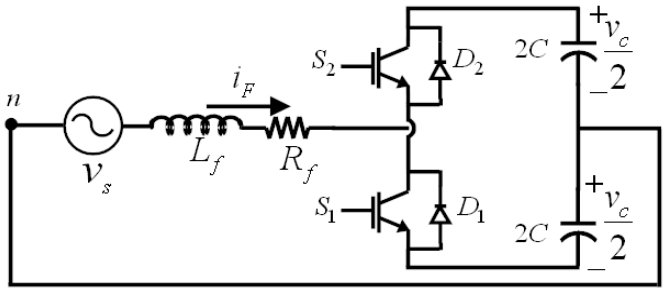

Fig.3 Equivalent Circuit structure for a single phase converter

simple and very easy to implement. An outer proportional-integral (PI) voltage loop is used to set the proper magnitude of the phase current and the choice of PI parameters (k_p, k_i) is based on the closed loop control as shown in Fig.2.In order to regulate the DC-link voltage v_{dc} , the error $v'_{dc} = v_{dcref} - v_{dc}$ is passed through the PI controller, which is given as

$$v_{dc} = k_p v'_{dc} + k_i \int v'_{dc} dt \tag{1}$$

From the Fig.2, the closed loop transfer function of DC-link voltage regulation, can be obtained as

$$\frac{v_{dc}(s)}{v_{dcref}(s)} = \frac{s + \frac{k_i}{k_p}}{s^2 + \frac{k_p}{C}s + \frac{k_i}{C}} \tag{2}$$

Where the proportional gain and integral gains are derived from $k_p = 2\delta\omega_n C$ and $k_i = C\omega_n^2$ .The outer loop natural frequency ω_n is considered as the fundamental frequency of the supply voltage.

3 Sliding Modes and Equivalent Control

The single phase Model of Fig. 3 does not take into consideration the shift in the voltage of the common capacitor node relative to the neutral of the source and this leads to a valid sliding-mode control law. If a switching function u is defined such that $u=1$ when either S1 or D1 is conducting, and $u=-1$ when either S2 or D2 is conducting, then the inductor current is given by

$$\frac{di_F}{dt}=\frac{v_s}{L_f}-u\frac{v_c}{2L_f}-\frac{R_f}{L_f}i_F \tag{3}$$

An expression for capacitor voltage taking into account the ripple due to compensating currents can be written as

$$\frac{dv_c}{dt}=-\frac{1}{2}[u_a\frac{i_{Fa}}{C}+u_b\frac{i_{Fb}}{C}+u_c\frac{i_{Fc}}{C}] \tag{4}$$

Where u_a , u_b , u_c are the independent controls for phases a, b, and c, respectively, and i_{Fa} , i_{Fb} , i_{Fc} are the compensating currents for phases a, b, and c, respectively. The filter can be

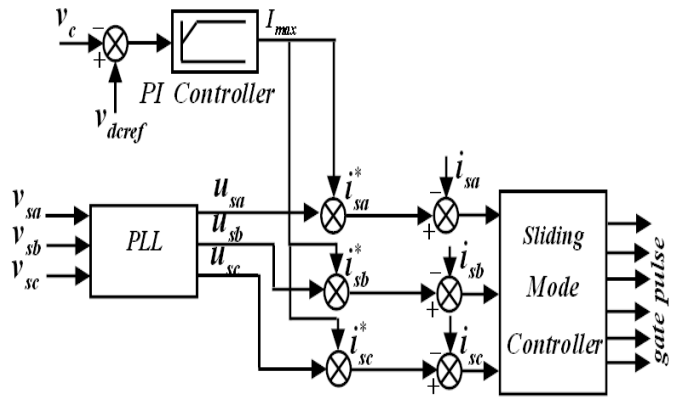

Fig.4 ICC Control Algorithm for SAPF

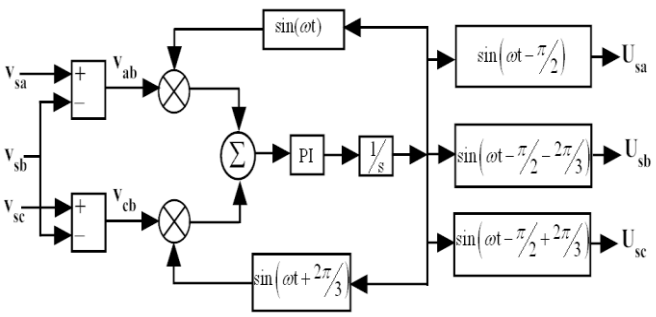

Fig.5 PLL structure diagram

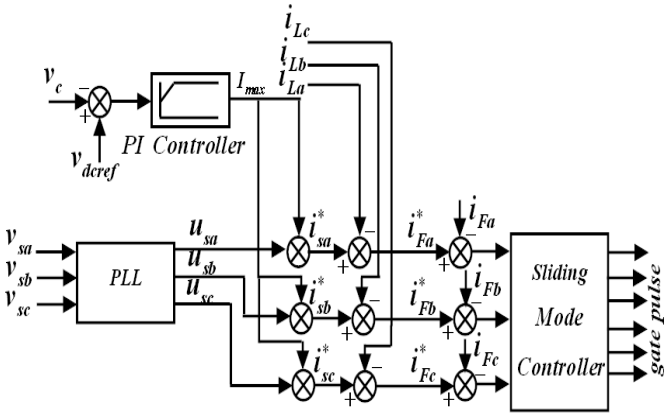

Fig.6 DCC Control Algorithm for SAPF

broken into three first-order independent systems which are expressed as

$$i_{sx}=i_{Lx}+i_{Fx} \tag{5}$$

$$=i_{Lx}+\int\left[\frac{v_{sx}}{L_f}-u_x\frac{v_c}{2L_f}-\frac{R_f}{L_f}i_{Fx}\right]dt \tag{6}$$

where x denotes the phase. To apply a sliding mode control theory to the active power filter, the sliding surfaces, or the trajectories, must be defined in such a way that we wish the system to follow. Here the trajectories are defined using the following two control strategies.

3.1 Indirect current control (ICC)

Fig.4 shows the ICC scheme for designing trajectory in SMC. Here the trajectories for line currents $i_{sa}^*, i_{sb}^*, i_{sc}^*$ are obtained by multiplying the unit vectors U_{sa}, U_{sb}, U_{sc} generated from phase locked loop (PLL), (shown in Fig.5.) with the continuous peak source current I_{sm} .

$$\begin{aligned} v_{sa}&=v_m\sin(\omega t)\\ v_{sb}&=v_m\sin(\omega t-120^\circ)\\ v_{sc}&=v_m\sin(\omega t+120^\circ)\end{aligned} \tag{7}$$

$$\begin{aligned} i_{sa}^*&=I_{sm}\times U_{sa}\\ i_{sb}^*&=I_{sm}\times U_{sb}\\ i_{sc}^*&=I_{sm}\times U_{sc}\end{aligned} \tag{8}$$

3.2 Direct current control (DCC)

Fig.6 shows the DCC scheme for designing trajectory in SMC. Here the trajectories for compensating currents $i_{Fa}^*, i_{Fb}^*, i_{Fc}^*$ are obtained by subtracting source reference currents from the load currents.

$$i_{Fa}^{*} = i_{sa}^{*} - i_{la}$$
$$i_{Fb}^{*} = i_{sb}^{*} - i_{lb} \quad (9)$$
$$i_{Fc}^{*} = i_{sc}^{*} - i_{lc}$$

The sliding surfaces are chosen according to ICC and DCC schemes and are given by,

$\mathbb{S}_x = [i_{sa}^{*} - i_{sa}] = 0$ (For Indirect Current Control)
$\mathbb{S}_y = [i_{Fa}^{*} - i_{Fa}] = 0$ (For Direct Current Control)

To assure that the system can be maintained on the sliding surface, it must be shown that there is a natural control which satisfies $\mathbb{S}\dot{\mathbb{S}} \le 0$ at all times, i.e., for all values that the state may experience. It u is within the natural control's bounds of the physical system for $\dot{\mathbb{S}} = 0$, and then it is possible to remain on the sliding surface at all times and maintain perfect tracking. Setting $\mathbb{S}_x = 0$ or $\mathbb{S}_y = 0$, the equivalent control can be found to be

$$u_{eqx} = \left(\frac{di_{Lx}}{dt} + \frac{v_{xn}}{L} - \frac{di_{sx}^{*}}{dt} - \frac{R_f}{L_f} i_{Fx} \right) \left(\frac{2L_f}{v_c} \right) \quad (10)$$

The natural control limits of the circuit are $-1 \le u_{eq} \le 1$. To satisfy $\mathbb{S}\dot{\mathbb{S}} \le 0$, the discontinuous control law can be seen

$$\text{If } \mathbb{S} < 0 \text{ then } u = 1 \quad (11)$$
$$\text{IF } \mathbb{S} > 0 \text{ then } u = -1$$

4 Simulation Results and Analysis

The control units have been tested using MATLAB-SIMULINK according to the structure shown in Fig.4 and Fig.6. A three phase diode bridge rectifier feeding RL load is considered as nonlinear load. The parameters used in the simulation are shown in Table 1, where R_f and L_f correspond to the link inductor model, C is the capacitance of dc bus, v_{dcref} is the reference DC bus voltage, K_P, K_i are the PI-controller constants, and V_{rms} is the rms value of the source voltage.

Table 1
(Simulation Parameters)

V_{rms}	360V	v_{dcref}	600V
R_L	6.6 Ω	R_f	1 Ω
L_L	22 mH	L_f	2.7mH
C	1800 μF	K_p	0.1273
R_s and L_s	0.1Ω and 0.1mH	K_i	4.5000

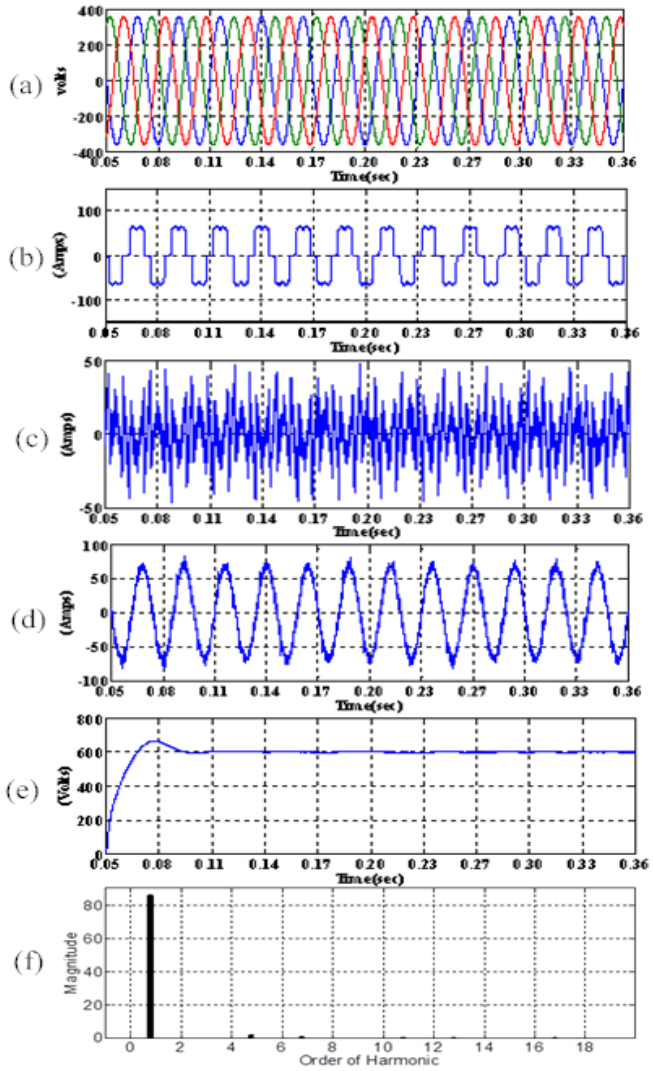

Fig.7 Simulation Waveform of the DCC with balanced supply condition (a)Source voltage (v_s), (b) Load current (i_{la}), (c) Compensation current (i_{fa}), (d) Source current (i_{sa}), (e) DC-link voltage (V_{dc}), (f) FFT of source current after compensation.

Investigations are carried out with three different operating conditions of source voltage such as balanced, distorted and unbalanced supply. A source voltage of 360V (rms) is considered for balanced supply condition and 4th order harmonic component is incorporated into the source voltage for the distorted supply condition. An unbalanced source voltage is created by phase variation to each other. A comparison is made between the both ICC and DCC under balanced, distorted and unbalanced source voltage condition. Figs.(7) - (8) show the performance of shunt active power filter under a balanced source voltage condition with DCC and ICC schemes respectively. The source voltage (v_s) ,load

current (i_{la}),compensation current (i_{fa}),source current (i_{sa}),DC-link voltage(v_{dc})and FFT of source current after compensation for phase-a are shown in these figures from top to bottom order.

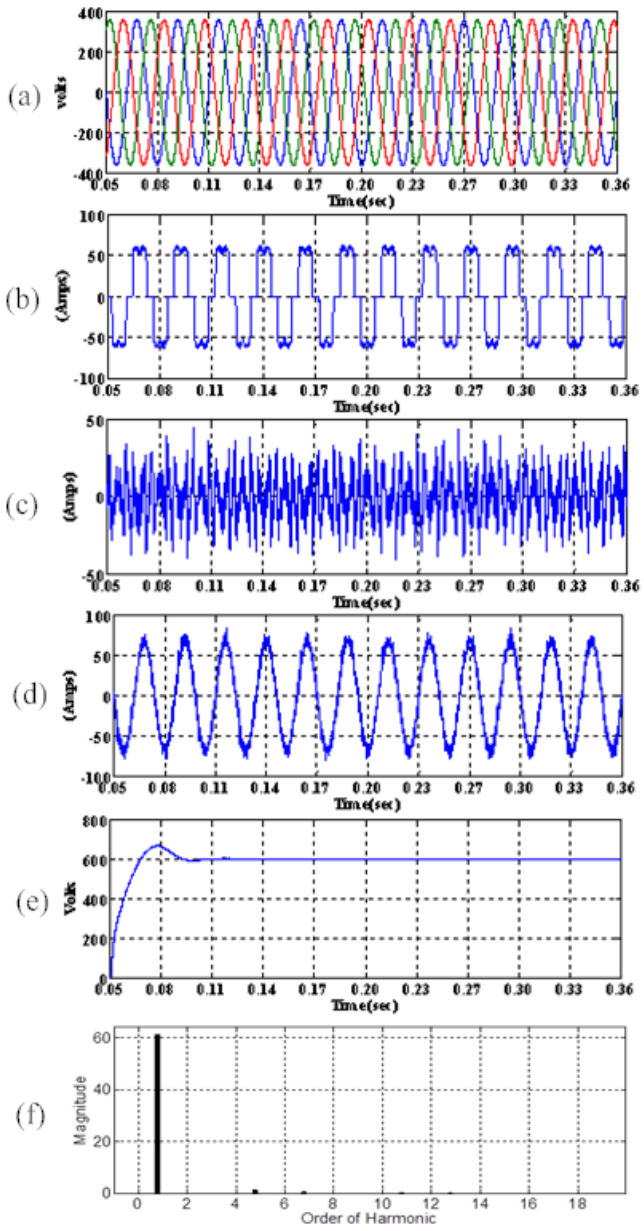

Fig.8 Simulation Waveform of the ICC with balanced supply condition, (a) Source voltage (v_s), (b)Load current (i_{la}), (c) Compensation current (i_{fa}), (d) Source current (i_{sa}), (e) DC-link voltage (V_{dc}), (f) FFT of source current after compensation.

From the Fig.7 (d) and Fig.8 (d), it is observed that the supply current is close to sinusoidal and remains in phase with source voltage therefore unity power factor is maintained. It is also observed that the DCC technique suffers from the switching ripples and results in a slightly high value of THD ($\approx$2.08%) in source current as compared to ICC technique ($\approx$ 1.87%), which is shown in Table 2.

Figs.9-10 shows the performance of SAPF under DCC and ICC with unbalanced source voltage conditions. It is observed from Fig.9 (d) and Fig.10 (d) that source current is

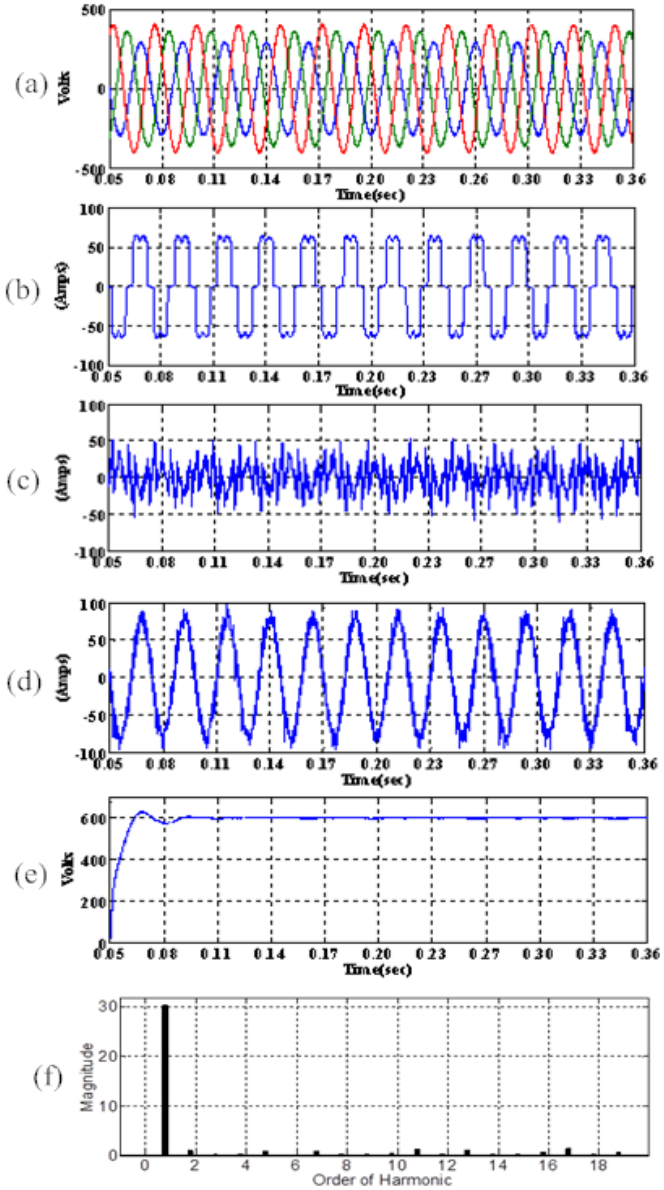

Fig.9 Simulation Waveform of the DCC with unbalanced supply condition, (a) Source voltage (v_s), (b) Load current (i_{la}), (c) Compensation current (i_{fa}), (d)Source current (i_{sa}), (e) DC-link voltage (V_{dc}), (f) FFT of source current after compensation.

sinusoidal and in phase with source voltage. But on the basis of calculation of THD, Table 2 shows the superiority of the ICC method (3.06%) over the DCC method (4.04%).

Figs.11-12 shows the performance of SAPF under DCC and ICC with the distorted source voltage condition with a similar order as in the above case. Here source voltage THD is taken as 8.14%, which is shown in Fig.11 (a). Source current results

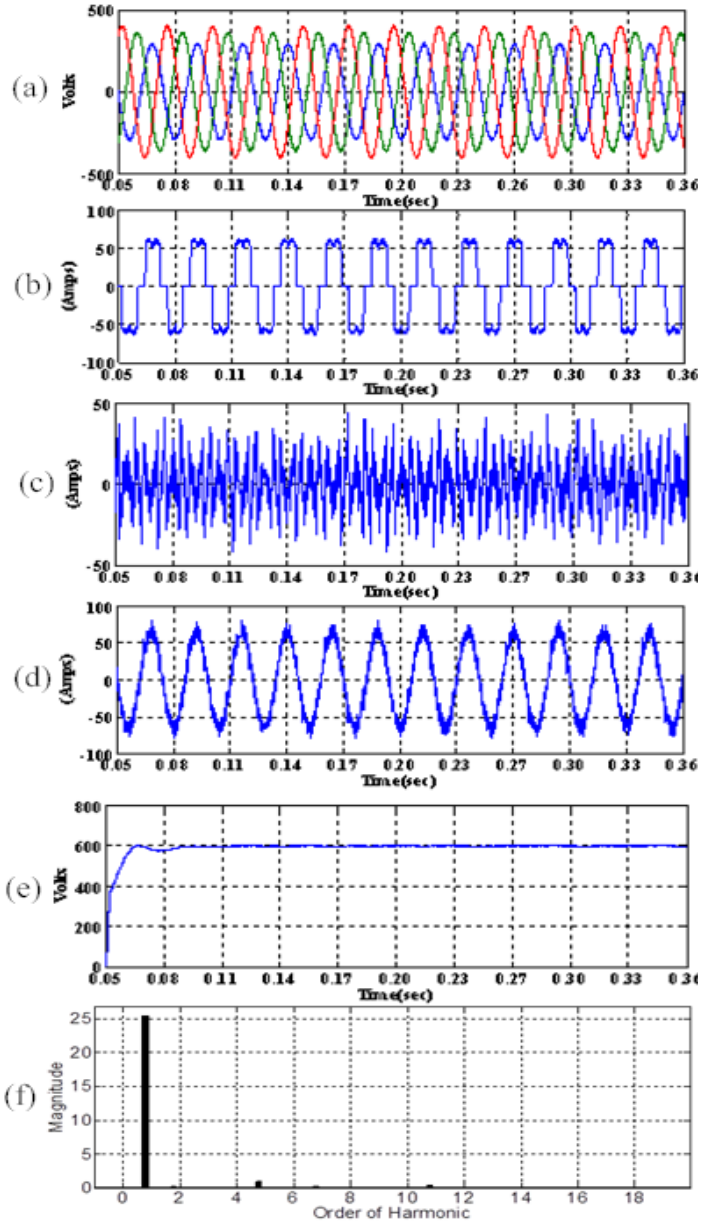

Fig.10 Simulation Waveform of the ICC with unbalanced supply condition, (a) Source voltage(v_s), (b) Load current (i_{la}), (c) Compensation current (i_{fa}), (d) Source current (i_{sa}), (e) DC-link voltage(V_{dc}), (f) FFT of source current after compensation.

(Fig.11 (d) and Fig.12 (d)) show the successful reduction of harmonics from the supply current by having on approximation of 4% THD. Table 2 shows that THD of DCC is found to be 4.60%, whereas in case of ICC it is 4.32%.

Amplitudes of different harmonic orders (5^{th} to 25th) for balanced source voltage condition are analysed using the above two methods, which are shown in Table 3, It can be found that the amplitude of harmonics is minimum in ICC as compared to DCC showing the higher priority of former one.

.

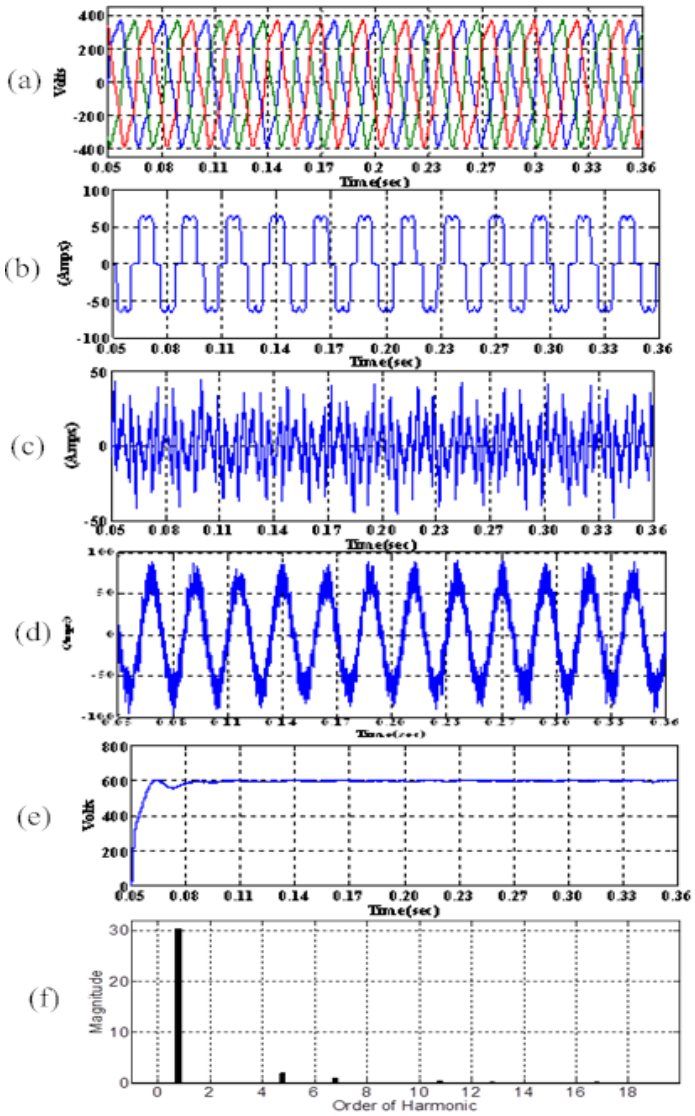

Fig.11 Simulation Waveform of the DCC with Distorted supply condition, (a) Source voltage (v_s), (b) Load current (i_{la}), (c) Compensation current (i_{fa}), (d) Source current (i_{sa}), (e) DC-link voltage (V_{dc}), (f) FFT of source current after compensation.

Table 2
(Calculation of THD %)

Source Voltage condition	Control Techniques	Source Current Before Compensation	Source Current After Compensation
Balanced Supply Voltage	DCC	29.71	2.08
	ICC	29.71	1.87
Unbalanced supply voltage	DCC	29.86	4.04
	ICC	29.86	3.06
Distorted supply voltage	DCC	30.11	4.60
	ICC	30.11	4.32

Table 3
Source current harmonics during balanced source-voltage condition

Harmonic order	DCC	ICC
5th	0.41	0.29
7th	0.44	0.27
11th	0.47	0.27
13th	0.36	0.29
17th	0.43	0.25
19th	0.41	0.26
23rd	0.46	0.31
25th	0.36	0.26

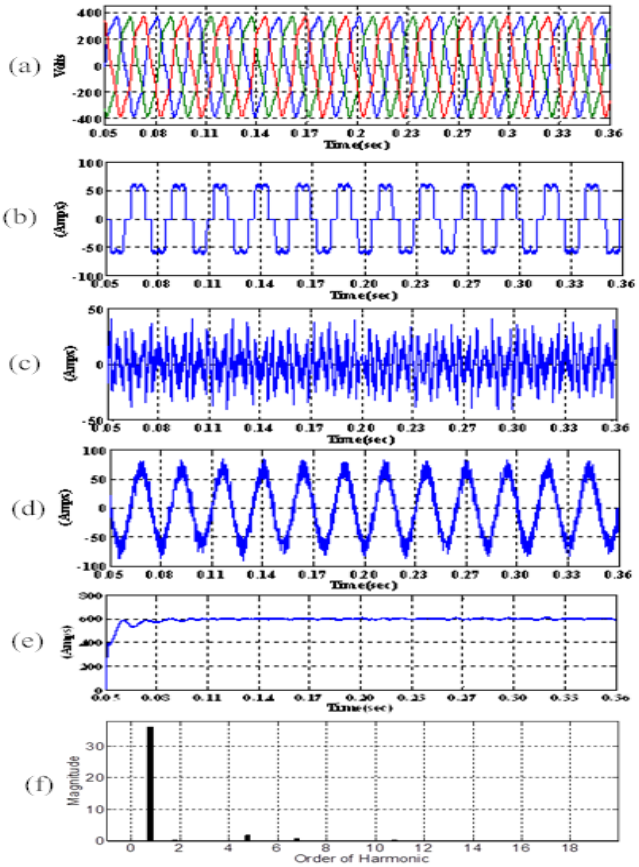

Fig.12 Simulation Waveform of the ICC with Distorted supply condition, (a) Source voltage(v_s), (b) Load current (i_{la}), (c) Compensation current(i_{fa}), (d) Source current(i_{sa}), (e) DC-link voltage(V_{dc}), (f) FFT of source current after compensation.

5 Validation with Real-time Digital Simulator

The Real-time digital simulator (RTDS) operates in real-time environment, therefore, not just allowing simulation of the power system, but additionally making it possible to test physical systems and control equipment. Fig.13 (a) demonstrates the Real-time execution of SAPF utilizing OPAL-RT it is comprised of the host computer, Real-time simulator and an oscilloscope. In host computer, simulink model edition, model compilation with RT-LAB and user interface is carried out. In target system, I/O and model execution process is carried out and the results are shown on an oscilloscope. OP5142 is one of the key foundations within the modular OP5000 input-output system from Opal-RT technologies which is shown in Fig.13 (b). It per permit the incorporation of FPGA in RT-LAB simulation clump for administering execution of hardware description language (HDL) capacities and high-speed, high-density digital I/O in real time modules. Based on the highest density Xilinx Spartan-3 FPGA, the OP5142 could be appended to the backplane of an I/O module of either a Wanda 3U and Wanda 4U based OPAL-RT simulation system. It communicates with the target PC through the PCI-Express ultra-low – latency real-time bus interface. The real-time digital verifications of SAPF under different supply conditions are shown in Figs. (14-19). The experimentation has

been carried out at switching frequency of 10kHz.Fig.14 illustrates the performance of SAPF under balanced supply condition, Fig.14 (a) provides information about the source voltage and Fig.15 (b) shows the waveforms of load current, compensation current, source current and DC-link voltage using DCC control scheme.Fig.15 follows the same pattern for ICC scheme. THD of DCC scheme is 2.11%, whereas THD of ICC scheme is 1.95%.Figs.16-17(a a b) and Figs.18-19(a & b) provide the results using unbalanced and distorted supply voltage conditions respectively. Here same sequence of waveforms is displayed as in the balanced case. From THD% analysis, it is found that source current THD in DCC scheme is 2.11% and in ICC scheme it is 1.95% using balanced condition. Also in unbalanced and distorted case, they are found to be (DCC=4.12%, ICC=3.13%) and (DCC=4.13%, ICC=3.15%) respectively. Finally a comparative assessment has been performed using MATLAB-SIMULINK and RTDS hardware as shown in Fig.20, and it is observed that the superiority of ICC over DCC under all operating conditions of supply voltage in SAPF.

(a)

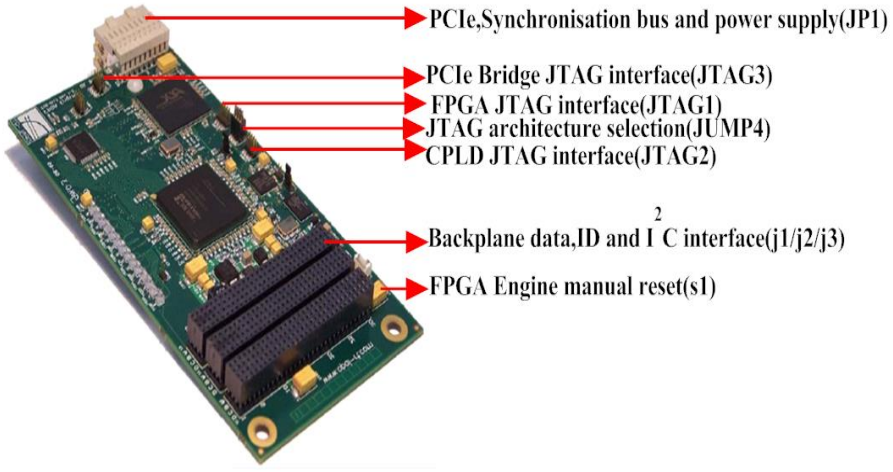

(b)

Fig.13 (a) Real-time implementation of SAPF control strategies using OPAL-RT (b) OP5142 layout and connection

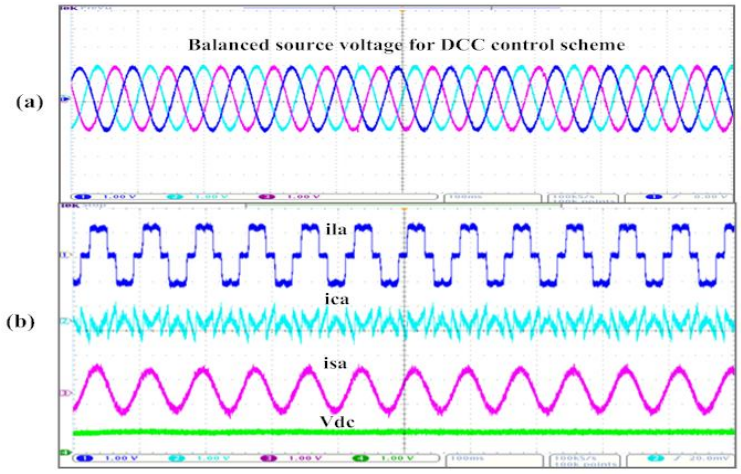

Fig.14(a) RT-lab real-time simulation waveform under Balanced supply for (a) source voltage (scale: 200v/div), (b) Load current (scale:55A/div), Compensation current (scale:35A/div), Source current (scale:66A/div), DC link voltage (scale:600v/div) for DCC Control schemes.

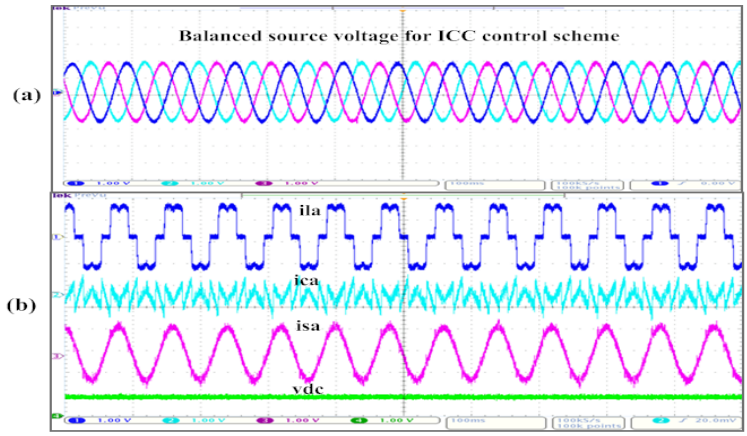

Fig.15(a) RT-lab real-time simulation waveform under balanced supply for (a) source voltage (scale: 200v/div), (b) Load current (scale:55A/div), Compensation current (scale:35A/div), Source current (scale:55A/div), DC link voltage (scale:600v/div) for ICC Control schemes

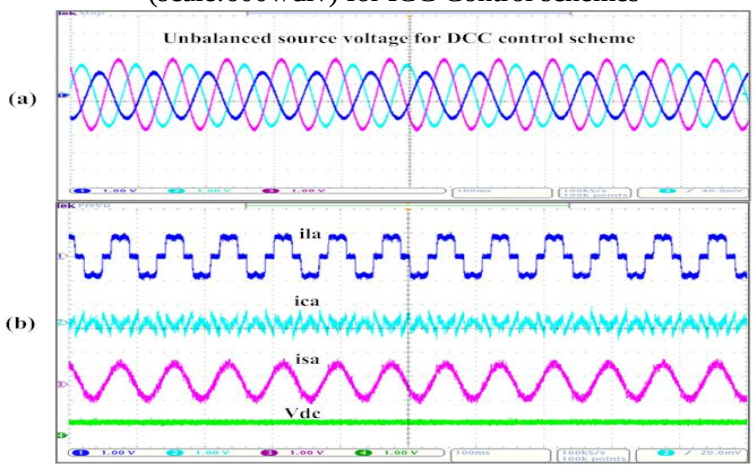

Fig.16(a) RT-lab real-time simulation waveform under unbalanced supply for (a) source voltage (scale: 200v/div), (b) Load current (scale:67A/div), Compensation current (scale:38A/div), Source current (scale:80A/div), DC link voltage (scale:600v/div) for DCC Control schemes

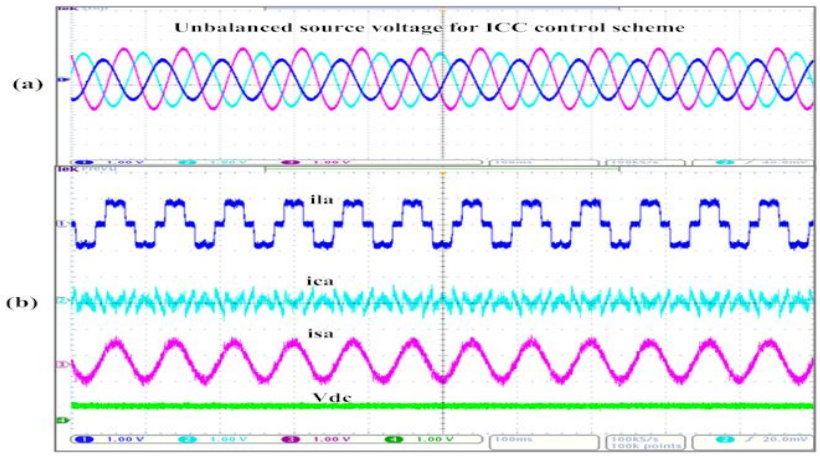

Fig.17(a) RT-lab real-time simulation waveform under unbalanced supply for (a) source voltage (scale: 200v/div), (b) Load current (scale:67A/div), Compensation current (scale:38A/div), Source current (scale:80A/div), DC link voltage (scale:600v/div) for ICC Control schemes

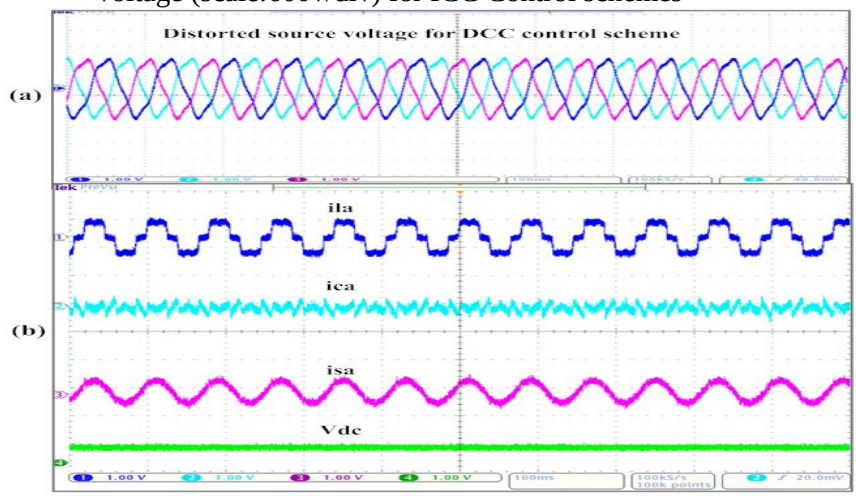

Fig.18(a) RT-lab real-time simulation waveform under distorted supply for (a) source voltage (scale: 200v/div), (b) Load current (scale:111A/div), Compensation current (scale:58A/div), Source current (scale:120A/div), DC link voltage (scale:600v/div) for DCC Control schemes.

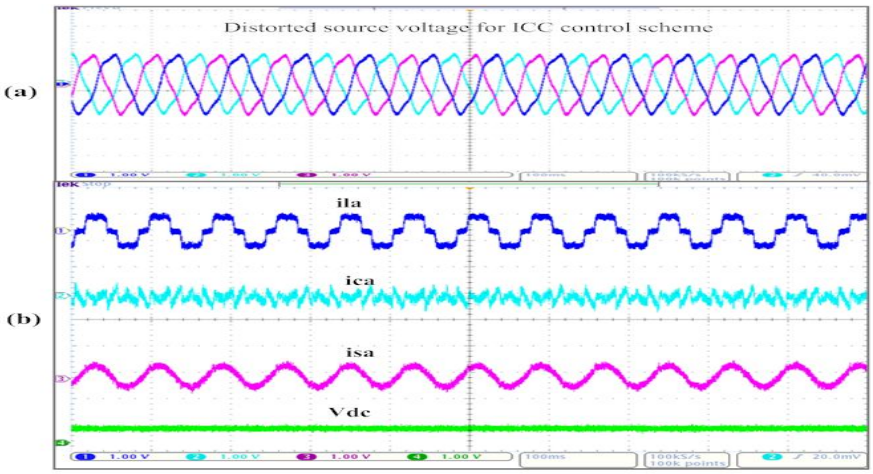

Fig.19(a) RT-lab real-time simulation waveform under distorted supply for (a) source voltage (scale: 200v/div), (b) Load current(scale:111A/div), Compensation current (scale:58A/div), Source current (scale:120A/div), DC link voltage (scale:600v/div) for ICC Control schemes

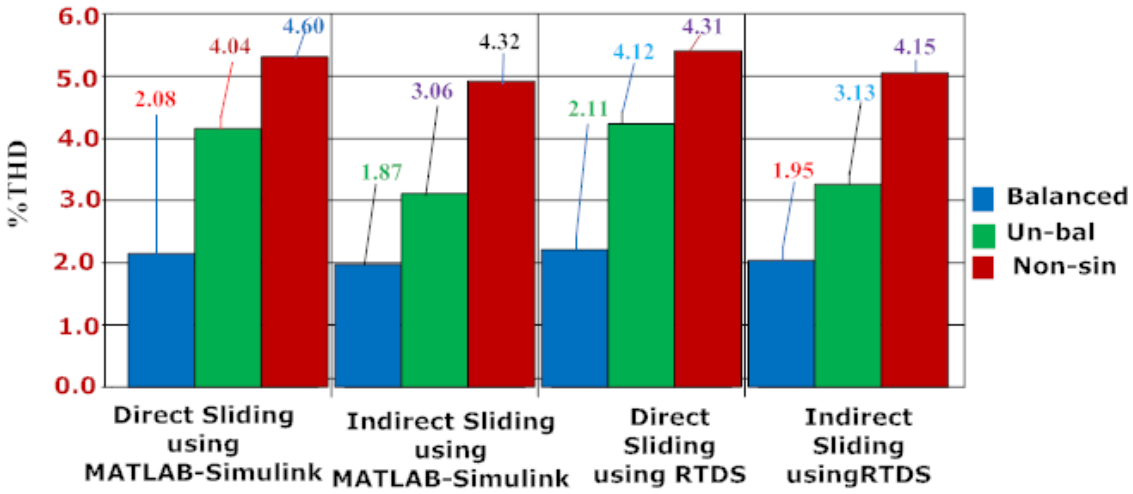

Fig.20 THD of Source Current for Direct sliding and Indirect sliding control strategies Using MATLAB-SIMULINK and Real-time digital simulator

6 Conclusion

The performance of Direct and Indirect current control strategies with the various supply conditions have been presented with sliding mode based SAPF.A novel sliding mode control is employed to reduce the reference current tracking error. The main benefit of utilizing a novel sliding mode controller to the SAPF with indirect current control strategy is that it doesn't have harmonic detection component and minimizes the harmonics for the massive amount of variation of load current under non-linear load conditions. In comparison with direct current control technique, it offers a simpler system structure and better harmonic compensating performances. The simulation and Opal-RT results exhibit an excellent harmonic compensation effect with the indirect current control method over the direct current control method with consideration of all possible conditions such as balanced, unbalanced and distortions in the supply side of SAPF.

References

[1] J. Matas, L. Garcia de Vicuna, J. Miret, J. M. Guerrero, and M. Castilla, "Feedback linearization of a single-phase active power," *IEEE Trans. on Power Electrons*, vol. 23, no. 1, p. 116–125, Mar. 2008.

[2] T. Thomas, and A. Jaffart, "Design and performance of active power filter," *IEEE Industry Applications magazine*, 1998.

[3] R. K. Patjoshi and K. K. Mahapatra, "Performance analysis of shunt Active power filter using PLL based control algorithms under distorted voltage condition," in *IEEE Students Conference* , MNNIT Allahabad, 2013, pp. 1-6.

[4] D. Stanciu, M. Teodorescu, A. Florescu, and D. A. Stoichescu, "Single-phase active power filter with improved sliding mode control," in *17th IEEE International Conference on Automation,Quality and Testing, Robotics (AQTR'10)*, May 2010, pp. 15-19.

[5] H. De Battista and R. J. Mantz, "Harmonic series compensators in power systems: their control via sliding mode," *IEEE Trans. on Control Systems Technology*, vol. 13, no. 1, pp. 133-138, Feb. 1998.

[6] B. Singh, A. Chandra, and K. Haddad, "A new control approach to three-phase active filter for harmonics and reactive power compensation," *IEEE Trans.on Power Systems*, vol. 13, no. 1, pp. 133-138, Feb. 1998.

[7] S. Rahmani, K.Haddad, "Experimental design and simulation of a modified pwm with an indirect current control technique applied to a single-phase shunt active power filter," *IEEE International Symposium on Industrial Electronics* , vol. 2, pp. 519-524, 2005.

[8] S. Buso, L. Malesani, P. Mattavelli, "Comparison of Current Control Techniques for Active Filter Applications," *IEEE Trans. On Industrial Electron*, vol. 45, pp. 722-729, Oct. 1998.

[9] Hu, Jiabing, et al, "Direct active and reactive power regulation of grid-connected DC/AC converters using sliding mode control approach," *IEEE Transactions on Power Electronics*, vol. 26, no. 1,

pp. 210-222, Jan. 2011.

[10] V. S. Bandal and P. N. Madurwa, "Performance analysis of shunt active power filter using sliding mode control strategies," in *12th International workshop on Variable Structure Systems*, March 2012.

[11] R. K. Patjoshi and K. K. Mahapatra, "Performance comparison of direct and indirect current control techniques applied to a sliding mode based shunt active power filter," in *India Conference (INDICON), 2013 Annual IEEE*, IIT Bombay, Dec. 2013, pp. 1-5.

[12] Saetieo, Suttichai, Rajesh Devaraj, and David A. Torrey, "The design and implementation of a three-phase active power filterbased on sliding mode control," *IEEE Trans. on Industry Applications*, vol. 31, no. 5, pp. 993-1000, Sep. 1995.

[13] BHUYAN, K. C., PATJOSHI, R. K., PADHEE, S., and MAHAPATRA, K., "Solid Oxide Fuel Cell with DC-DC Converter System: Control and Grid Interfacing," *WSEAS Transactions on Systems & Control*, vol. 9, 2014.

[14] ABDELKRIM, T., B, K., BENSLIMANE, T., and BENKHELIFA, A, "Stabilization of DC Link Voltage Using Redundant Vectors for Five-Level Diode Clamped Shunt Active Power Filter," *WSEAS TRANSACTIONS on CIRCUITS and SYSTEMS*, vol. 12, no. 5, pp. 151-160, May 2013.

[15] POORNASELVAN, R. S SUNDARAM K J, and N. DEVARAJAN, "Matlab Simulation of Sliding Mode Control of Shunt Active Filter for Power Quality Improvement", *WSEAS TRANSACTIONS on CIRCUITS and SYSTEMS,2014.*

[16] G. K. Singh, A. K. Singh, and R. Mitra, "A simple fuzzy logic based robust active power filter for harmonics minimization under random load variation," Electric Power Systems Research, vol. 77, no. 8, pp. 1101–1111, 2007.

[17] Ghasemi A. ,. Mortazavi S. S.and Kianinezhad. R., "Fuzzy logic controlled adaptive active power filter for harmonics minimization and reactive power compensation under fast load variation," *WSEAS Transactions on Power Systems* , vol. 3, no. 5, pp. 300-309, May 2008.

[18] AREERAK K.L.,Areerak T. N.,"Shunt Active Power Filter Design using Genetic Algorithm Method," *WSEA Transactions on Systems* , vol. 9, no. 4, pp. 327-336, Apr. 2010.

[19] SARAVANAN P. ,BALAKRISHN P.A.,"An Efficient BFO Algorithm for Self Tuning Pi-Controller Parameters for Shunt Active Power Filter," *WSEAS TRANSACTIONS on Power System*, vol. 9, pp. 155-170, 2014.

[20] Moran L. A.,Fern´andez L.,Dixon J.W. and Wallace R.,"A simple and low-cost control strategy for active power filters connected in cascade," *ndustrial Electronics, IEEE Transactions*, vol. 44, no. 5, pp. 621-629, Oct. 1997.